Journal of Natural Gas Science and Engineering 35 (2016) 826–835

Contents lists available at ScienceDirect

Journal of Natural Gas Science and Engineering

journal homepage: www.elsevier.com/locate/jngse

Formation damage during alkaline-surfactant-polymer flooding in the Sanan-5 block of the Daqing Oilfield, China

Zihao Li [a, d, e], Wei Zhang [b], Yongqiang Tang [a, d, e], Baiguang Li [c], Zhaojie Song [a, d, e], Jirui Hou [a, d, e, *]

[a] Enhanced Oil Recovery Institute, China University of Petroleum (Beijing), Beijing, 102249, China
[b] China HuaYou Group Corporation, China
[c] No.2 Oil Production Company, Daqing Oilfield Limited Company, Daqing, 163414, China
[d] Basic Theory Laboratory of Improving Oil Recovery in Low Permeability Oilfields, Tertiary Oil Recovery Key Laboratory, CNPC, Beijing, 102249, China
[e] Key Laboratory of Petroleum Engineering, Ministry of Education, Beijing, 102249, China

ARTICLE INFO

Article history:
Received 29 March 2016
Received in revised form
19 July 2016
Accepted 21 July 2016
Available online 25 July 2016

Keywords:
ASP flooding
Formation damage
Permeability
Porosity

ABSTRACT

Alkaline-Surfactant-Polymer (ASP) flooding is an emerging chemical Enhanced Oil Recovery (EOR) technology which has significantly enhanced oil recovery of Daqing Oilfield. ASP flooding benefits from the synergy effects of alkali, surfactant and polymer to improve both volumetric and displacement efficiencies and meanwhile lower surfactant adsorption. However, ASP flooding also induces some negative formation damage effects such as scaling, adsorption, and mineral dissolution. In this paper, we investigated the formation damage caused during ASP flooding in Block Sanan-5 in Songliao Basin – one of the most productive blocks of Daqing Oilfield in China.

It was found that the distribution of formation damage caused by ASP flooding followed flow paths of chemical solutions and was dependent on well locations. The severity of damage varies as distance increases from the near-injection-well area to the near-production-well area. Understanding the effects of well locations on formation damage during ASP flooding could provide more accurate evaluation of formation damage and helped to guide reservoir development strategies. To analyze the well location factor, we collected scaling samples and more than 970 m of core samples from Block Sanan-5 of Daqing Oilfield covering different wells on various flow paths before and after ASP flooding. The changes of some key petrophysical parameters such as porosity and permeability before and after ASP flooding were investigated. A series of experiments, including Scanning Electron Microscopy (SEM), Casting Thin Sections (CTS), X-Ray Diffraction (XRD) and ion analysis of produced water were performed to test properties of core samples. In addition, absorption of different components in the ASP solutions was also measured.

Experimental results indicate that the ASP flooding has considerably different influences on different parts of flow paths. After ASP flooding, permeability distribution of core samples exhibits different variability trends from the near-injection-well areas to near-production-well areas. Due to absorption of alkali and polymer, grains migration and scaling of calcium and magnesium, permeability decreases at the near-injection-well area, then increases at an intermediate distance and decreases again at the near-production-well. Moreover, porosity of samples shows a similar tendency with variability of permeability, which is interpreted by the strong mineral corrosion due to high concentration of alkali in the near-wellbore area, while its extent of variation is smaller than permeability.

1. Introduction

Chemical flooding using an alkaline-surfactant-polymer (ASP) is a flexible technique that is applicable to many reservoirs. The research on this subject is comprehensive and meticulous (Wang et al., 2014; Denney, 2013; French, 1996; Duan et al., 2014; Zhang

* Corresponding author. Enhanced Oil Recovery Institute, China University of Petroleum (Beijing), Beijing, 102249, China.
E-mail address: jiruihou@cup.edu.cn (J. Hou).

http://dx.doi.org/10.1016/j.jngse.2016.07.046
1875-5100/

et al., 2016; Tang et al., 2013; Korrani et al., 2016). In brief, surfactants lower the water-oil interfacial tension so that isolated oil is mobilized and remove the residual oil film, the alkali forms soap with acidic crude oils and lowers the surfactant adsorption, and the polymers increase the viscosity of the aqueous phase, pulling out bypassed oil and reducing bypassing (Pope et al., 1979). Due to the alkaline agents and other ions in the ASP fluid that are incompatible with the reservoir, some reactions will occur during the migration of the ASP fluid (Wang and Wang, 2003). Considering the distance between wells, the reactions and mechanisms occurring during the fluid migration are not all of the same, varying from the injection well areas to production well areas, such as:

$$KAlSi_3O_8 + Na_{1-x}Ca_x[Al_{1+x}Si_{3-x}O_8] + OH^- \rightarrow Al(OH)_3\downarrow + K^+ + Na^+ + Ca^{2+} + SiO_3^{2-} \quad \text{(I)}$$

$$SiO_2 + 2OH^- \rightarrow SiO_3^{2-} + H_2O \quad \text{(II)}$$

$$Ca^{2+} + 2OH^- \rightarrow Ca(OH)_2\downarrow \quad \text{(III)}$$

$$Na^+ + AlO_2^- + 3SiO_3^{2-} + 3H_2O \rightarrow NaAlSi_3O_8 + 6OH^- \quad \text{(IV)}$$

Therefore, various effects on the reservoir properties, such as permeability and porosity, could occur through these reactions and mechanisms in the entire flowing path area. Oil recovery by ASP flooding benefits from some of these reactions and mechanisms above.

However, some other the reactions and mechanisms may not enhance the oil recovery. These include chromatographic separation (Hao et al., 2015; Liu et al., 2015), adsorption and retention (Volokitin et al., 2014; Li et al., 2001), corrosion (Wu et al., 2015; Alwi et al., 2014a,b; Rathnaweera et al., 2015; Ciantia et al., 2015), changing mineral composition (Li et al., 2015; Wang and Wang, 2003), grain migration (Yuan et al., 2015) and scaling problems (Denney and Others, 2008; Karazincir et al., 2011; Wang and Cheng, 2003; Yuan et al., 2011). The previously noted roles of alkaline agents, are attributed to their ability to increase the pH (Kazempour et al., 2012). Simultaneously injecting a chemical displacing fluid containing alkali into a reservoir may lead to silicate mineral dissolution, secondary mineral precipitation and even mineral migration possibly resulting in changes of permeability and porosity (Yuan et al., 2016). Numerous experiments have been published on mineral dissolution in silicate minerals (Fu et al., 2009). Sydansk (1982) studied the interaction of a sodium hydroxide solution with sandstone at elevated temperature and found the following: (a) significant dissolution silicate minerals, (b) sandstone weight loss, (c) increased porosity, (d) propagation of significant concentrations of water-soluble silicates, (e) in situ formation of new immobile aluminosilicate materials, (f) changes in permeability and (g) hydroxide ion consumption. Numerous researchers have reported that mineral dissolution and precipitation reactions in the subsurface porous media can alter the structure of the pore network and may impact porosity, permeability and flow paths (Cai et al., 2009; Colon et al., 2004; Crandell et al., 2012; Emmanuel and Berkowitz, 2005; Um et al., 2005). Therefore, alkaline agents play an important role in formation damage to the reservoir caused by ASP flooding and directly influence the degree of damage in the different locations in the flow pathway.

It is important to understand the effects of ASP flooding because ASP flooding affects the reservoir in ways that differ from water flooding (Wang, 2001a,b, 2003). Hou (2005) studied the synthetic effects of an ASP solution on the interfacial and rheological properties on displacement oil using an interface tensiometer and rheometer; Sedaghat et al. (2015) used pore-level experimental investigation to evaluate ASP formulations for heavy oil; Li et al. (2014) researched the adsorption properties of an ASP flooding system in the central Saertu sub reservoir in Daqing by static core adsorption experiments and dynamic core flooding experiments; Kalwar et al. (2014) designed a new approach for ASP flooding in high saline and hard carbonate reservoirs. He et al. (2015) studied reservoir pore-throat structural changes after strong base ASP flooding in the Daqing oilfield through mercury injection, scanning electron microscopy (SEM) and casting thin section (CTS) analysis; Kumar and Mohanty (2010) reported on a selected alkaline-surfactant system for viscous oil that was tested in a sand pack flood; Jia et al. (2006) studied the factors influencing the ASP displacement efficiency in the Daqing Oilfield using a micro-displacement experiment. Weatherill (2009) studied surface development aspects of ASP flooding. Farajzadeh et al. (2013) researched effect of continuous, trapped, and flowing gas on performance of ASP flooding. The results from a large numbers of investigations on related topics have been reported through the laboratory experiments noted above. However, the former relevant formation damage studies mainly focused on the laboratory simulations rather than field pilot testing. Because the limited laboratory simulations could not be compared with the entire reservoir in scale, analyzing core samples from different positions in the flow pathway would be more comprehensive. Therefore we collected more than 3000 feet of core samples from the Sanan-5 Block of the Daqing Oilfield, from areas of injection, production and inspection (located in the middle of flow path) well areas to discover whether the distribution of formation damage caused by ASP flooding follows the flow paths of chemical solutions and is dependent on well locations.

2. Geologic setting and production history

The Songliao Basin, the largest oil production base in China, is a large-scale Mesozoic and Cenozoic continental sedimentary basin situated in the northeastern China (119°40′-128°24′ E longitude and 42°25′-49°23′ N latitude). It is 750 km long and approximately 350 km wide, extending through three provinces of China, with total area of 260,000 km^2 (Fig. 1A) (Wei et al., 2010; Zhao et al., 2011).

The Daqing placanticline, a typical inversion structure, is located in the central depression of the Songliao Basin. It is approximately 140 km long from south to north and from 6 to 30 km wide. The top of this structure is 1050 m below sea level, the thickness and its area are 524 m and 2800 km^2, respectively (Fig. 1B).

The Saertu Oilfield is located in the middle of the Daqing placanticline. The length from south to north of this oilfield is 32 km, the width in northern part of the oilfield is 20 km and 12 km in the southern part. The oil-bearing area is approximately 200 km^2. The oil-bearing reservoir is in the Lower Cretaceous strata that includes the Qingshankou, Yaojia and Nenjiang formations (Fig. 1B) (Li Mingyuan, 2009).

The Sanan-5 Block is located to the south of Saertu anticline and Line-30 and north of Line-3 Sanan-4 area, and it reaches the boundaries of the Putouhua II oil reservoir in the east and west. The oil-bearing area is approximately 12 km^2. The average dip angle is 3.7° in the east and 18.5° in the west (Li Chen, 2010).

The depth of the oil-bearing strata in the Sanan-5 Block ranges from 775 to 1196 m. These include the Saertu, Putaohua and Gaotaizi strata and are divided into 41 sandstone layers and 130 substratum layers. The effective thicknesses of the oil-bearing strata are approximately 60 m in the center, 30 m in the south, and 40 m in the north of the oilfield (Li Chen, 2010).

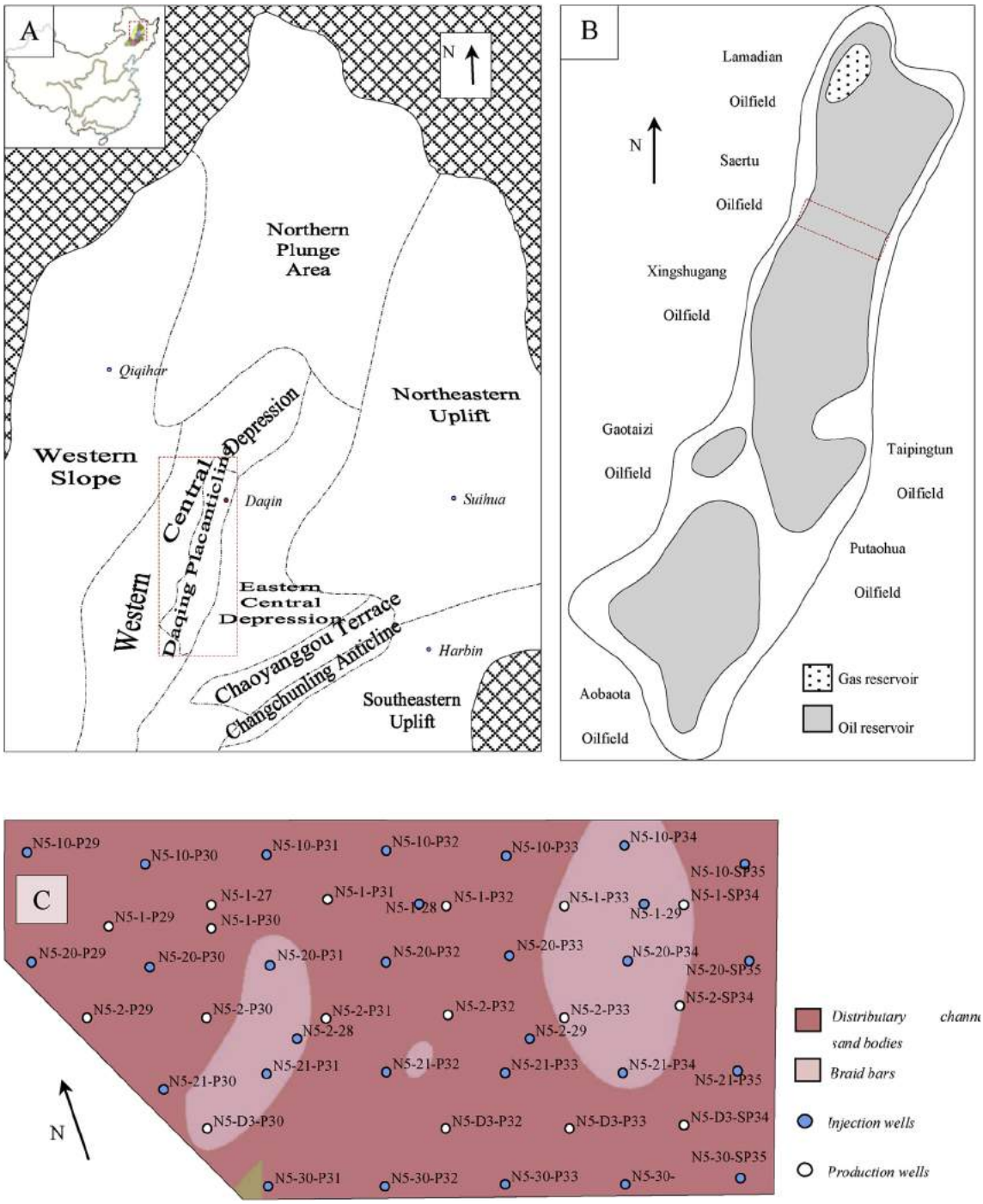

Fig. 1. The geology survey of Daqing oilfield (A, B) and ASP pilot test field of block Sanan-5 (C).

Beginning in 1965, 117 wells (46 production and 71 injection) were drilled in the Sanan-5 Block (in the Saertu, Putaohua and Gaotaizi strata) using a linear well pattern with a well spacing of 300 m and a line spacing of 500 m.

In 1984, 146 infill wells (97 production and 49 injection) were drilled to adjust the injection-production program into an invert nine-spot pattern with an average well spacing of 250 m to exploit the low and middle permeability layers.

In 1996 the injection-production program was adjusted again as 252 wells (162 production and 90 injection) were drilled, constructing a five-spot water flooding system. The number of wells in the Sanan-5 Block had reached 519, and the well pattern density was 43.2 wells per kilometer (Li Chen, 2010).

In 2005, the application of ASP flooding in Daqing oil field entered the experimental phase. A section in the western part of the Sanan-5 Block was selected as the ASP flooding experimental area. The target zone is approximately 2.4 km^2 (Fig. 1C). The total pore volume is 657.3 $\times$ 10^4 m^3, and its geological reserve is approximately 310.4 $\times$ 10^4 t. This major reservoir stratum is designated Putaohua I 1–2 and has a nominal thickness of 13 m and an effective thickness of 9.4 m (Sun, 2011).

3. Methodology

3.1. Porosity and permeability measurement

The porosity and permeability are the key parameters of the reservoir. The variation of porosity and permeability before and after ASP flooding directly effects the flow characteristics of reservoir. A total of 125 core samples were obtained, consisting of 20 before and 105 after ASP flooding. The after-ASP core samples consisted of 35 from injection wells, 35 from inspection wells in the middle and 35 from production wells.

Due to their scarcity, the before-ASP core samples were directly provided by the first party. The after-ASP core samples were obtained from the similar layer and burial depth of 970–980 m. All of the core samples before and after ASP flooding were obtained from the same stratigraphic unit and they all belonged to single sand body of underwater branched river channel during the same geological period.

The porosity of the core samples was determined using a Model HKXD-C Helium Porosity Automatic Analyzer and the permeability was determined using a Model DYX-2 Full Diameter Core Permeability Analyzer. Both of these analyzers were manufactured by the Haian County Petroleum Scientific Instrument Co., LTD. The results from both of these analyzers were automatically computed by corresponding software. The equipment manufacturer states that the error ranges of porosity and permeability measurements are within 0.5% and 5%, respectively.

3.2. Adsorption of ASP fluid

The adsorption of the ASP constituents onto the rock surface directly influences the oil displacement performance and the reservoir properties. Therefore, the adsorption and desorption characteristics are worth researching. Due to the high concentration of ASP fluid, the laboratory experimental simulations are similar to the situation in the injection well areas. Therefore, core samples from before and after ASP flooding were selected to perform an experiment.

Eight core samples in the injection well after ASP flooding were used to test their adsorption capacity for the ASP constituents. The cores were smashed and washed by recirculating the alcohol mixture to dissolve the ASP constituents. The NaOH was determined using a Thermo pH meter, the heavy alkylbenzene sulfonate (HABS) concentration was determined using an LC-20A liquid chromatograph at 35 °C, and the polyacrylamide (PAM) concentration was determined using an ultraviolet spectrophotometer.

Eight before ASP-flooding cores were used to simulate the adsorption process and to test their adsorption capacity. The ASP system consisted of 1% alkali, 0.3% HABS and 0.15% HPAM. After cleaning with mixture of 25% alcohol and 75% methanol, the cores were saturated with water under vacuum and then immediately flooded with the ASP fluids. Along with the displacement volume, the produced liquid was collected and quantitatively analyzed in real time to determine the concentrations of the ASP constituents.

3.3. Scaling and microstructure

To investigate the changes of porosity and permeability, the microstructure and mineral composition of the core samples were analyzed. In addition, scaling problems have a serious influence on oilfield equipment and may have negative effects on production. The type and quantity of scaling can also predict the reactions that occur.

The microscopic features of the core samples and scaling samples were observed using CTS, SEM, and mineral components were tested by X-ray diffraction (XRD) methods, all following related testing standards.

4. Results and discussion

4.1. Permeability and porosity

The results of permeability and porosity measurements of the core samples before and after ASP flooding are shown in Figs. 2 and 3, respectively, and the relationship between these two parameters is shown in Fig. 4.

As seen in Figs. 2–4, the porosity values of all of the core samples were largely limited to the range of 23%–30%. Except a few of cores from production wells, the porosity values of the cores after ASP flooding generally were higher than those of the cores before ASP flooding (Fig. 2). However, the distribution of the Klinkenberg-corrected permeability values was mainly from 100×10^{-3} μm^2 (0.1 D) to 4000×10^{-3} μm^2 (4 D), although some of the cores might have been taken from the interlayers (low permeability) or fractures (high permeability). The permeability values of the cores obtained from different types of wells showed different distributions (Fig. 3). In general, the permeability values of cores from inspection wells in the middle areas were relatively the highest, the cores from the injection wells were generally lower than those of the inspection wells and cores from production wells generally had the lowest permeability values (Fig. 4).

Compared with the cores before ASP flooding, the permeability values of cores after ASP flooding in every localized area presents different trends. In brief, the permeability values of cores before ASP flooding were higher than those of after ASP flooding cores for the injection and production wells, but lower for the inspection wells in the middle area. We hypothesized that the reasons that this occurred were related to many mechanisms that occurred when the ASP fluid migrated from the injection well areas to the production well areas. This hypothesis was verified through the series of experiments described below.

4.2. Adsorption

The result of adsorption of after-ASP core samples is shown in Table 1.

It is the example of ASP contention curves. For three detections, each sample should be no less than 3 mL.

In the produced water of first sample, only polymer was detected and its concentration was 4.12% of the initial value, and its adsorption was weakest throughout. Compared with the surfactant, the adsorption of the alkali was relatively weak, albeit it was a

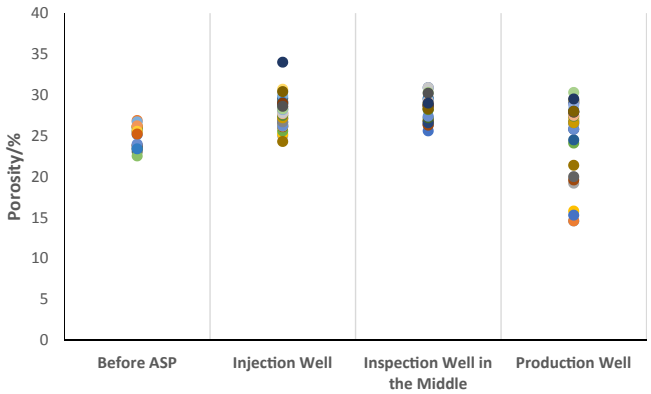

Fig. 2. Porosity of the core samples before and after ASP flooding.

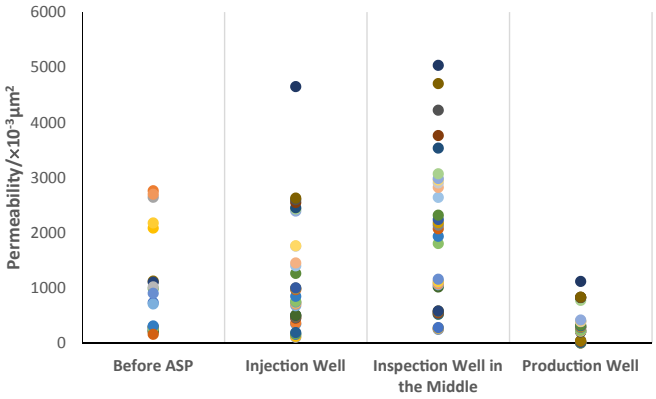

Fig. 3. Permeability of the core samples before and after ASP flooding.

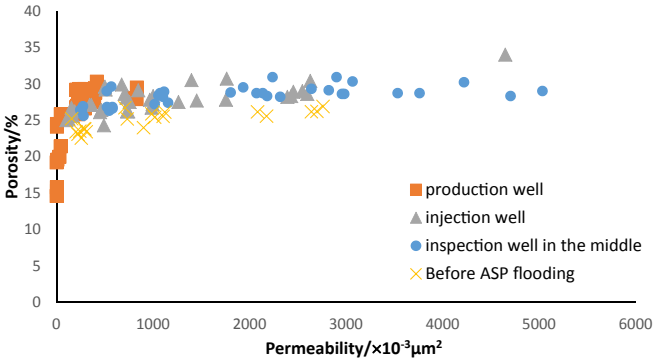

Fig. 4. Porosity and permeability of the core samples before and after ASP flooding.

Table 1
Adsorption of core samples after ASP flooding.

No.	Alkali content (g/g)	HABS content (g/g)	PAM content (g/g)
1	2.098E-07	1.28E-04	2.22E-04
2	4.284E-07	2.00E-04	3.94E-04
3	9.372E-07	1.73E-04	2.40E-04
4	4.919E-07	1.38E-04	4.13E-04
5	7.796E-07	1.68E-04	9.07E-04
6	4.486E-07	1.47E-04	4.08E-04
7	9.814E-07	1.58E-04	3.64E-04
8	5.519E-07	1.77E-04	7.00E-04

The result of simulating the process of adsorption and testing the adsorption capacity from before-ASP core samples are shown in Fig. 4.

sacrificial agent.

After the injection volume reached approximately twenty times the column volume, the composition of the produced fluids was the same as ASP flooding fluid. The cumulative retention was approximately calculated (in Table 2). Subsequently, the cores were water flooding in reverse to remove the ASP constituents, and the extracted fluids were analyzed for the ASP constituents to determine the amount of adsorption. Next, the cores were smashed and washed with the alcohol mixture to dissolve the adsorbed constituents. Except for the ASP in the pores, the summation was approximately the quantity that was physically adsorbed (in Table 2).

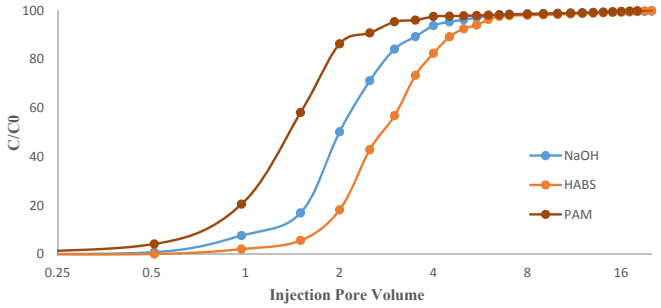

Fig. 5. Simulating the process of adsorption of ASP flooding.

The result indicated that the adsorption capacity of PAM was large, but its permanent adsorption was small. Instead, the adsorption of alkali was weaker, but the permanent adsorption of alkali was the strongest. A possible reason was that part of the adsorption of alkali was chemical adsorption which is usually an irreversible process. The fact that the adsorbed surfactant and polymer could be washed out means they are mainly physically adsorbed.

The adsorption of the ASP fluid will influence the residual resistance factor (Cheng et al., 1992). Although alkali reduces the adsorption of the surfactant as a sacrificial agent, the adsorption of polymer still remains at a level that is higher than other two constituents. There was no doubt that the adsorbed polymer would influence the permeability of reservoir.

4.3. Microstructure

Sixteen polished and resin-filled CTS were analyzed to cover the full range of the streamline. CTS could not only be applied to differentiate the minerals but also to keep the mineral granules pristine, which was helpful in identifying the formation damage caused by ASP flooding. Various types of clays were the most common minerals associated with formation damage. Within the pore system, the type and the location of clay minerals were both important and significant.

Viewed under plane-polarized (−) and crossed-polarized (+) light, as shown in Fig. 5, it was observed that the dominate grain frameworks were quartzes and loose feldspars. Among the

Table 2
Quantity of physically adsorption.

No.	Alkali content (g/g)		HABS content (g/g)		PAM content (g/g)	
	Adsorption	Dissociation	Adsorption	Dissociation	Adsorption	Dissociation
1	3.31E-05	1.03E-07	1.92E-04	9.45E-05	1.66E-04	1.07E-04
2	2.57E-05	5.39E-08	1.24E-04	3.40E-05	7.29E-05	6.79E-05
3	1.26E-05	4.19E-08	4.94E-05	2.42E-05	4.05E-05	2.57E-06
4	2.95E-05	8.16E-08	1.10E-04	6.13E-05	9.31E-05	7.72E-05
5	2.69E-05	7.98E-08	9.97E-05	4.70E-05	7.58E-05	7.02E-05
6	4.68E-05	1.32E-07	2.65E-04	1.08E-04	1.51E-04	1.38E-04
7	5.89E-05	1.96E-07	3.13E-04	1.24E-04	2.31E-04	1.87E-04
8	5.62E-05	1.45E-07	2.95E-04	1.13E-04	2.69E-04	1.82E-04

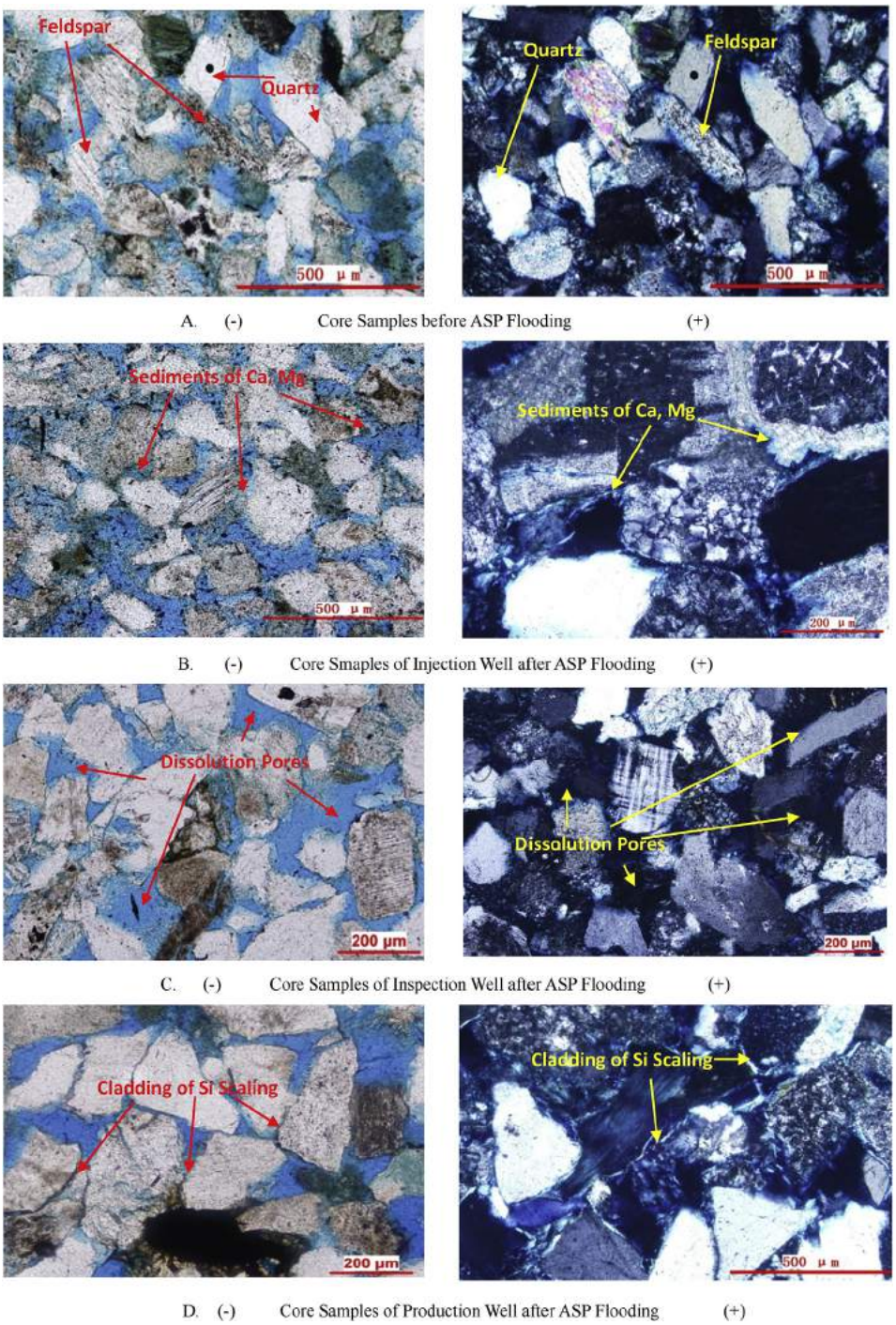

Fig. 6. CTS of core samples before and after ASP flooding.

minerals, dot-line contact was the major form of the connection between the sediment granules. In the samples before ASP flooding (Fig. 5A), the pore-throat distribution was uneven. The detrital grains contained quartzes and feldspar clastic particles and the pore type was mainly an intergranular dissolved pore. Then, near the injection wells after ASP flooding (Fig. 5B), on the cementation and grain surfaces, corrosion was strong and some throats were plugged by sediment. Moreover, near the core samples of the inspection wells (Fig. 5C), the corrosion of cementation and part of feldspars was less and the pore-throat connectivity was better because less new sediment was formed contributing to the increase of permeability. Finally, for the core samples from production wells (Fig. 5D), some detrital grains were slightly corroded and there was partial sedimentation on the surface of grains, including silicon scale and chlorite, forming a coating to block the pores-throats and decreasing the connectivity.

In order to visually determine the formation damage, SEM analysis (Fig. 6) was simultaneously performed for contrastive analysis of before and after ASP flooding.

The microscopic features of the core samples before ASP flooding (Fig. 7A) included an uneven distribution of pores and throats and strong heterogeneity. In addition, cementation filled in

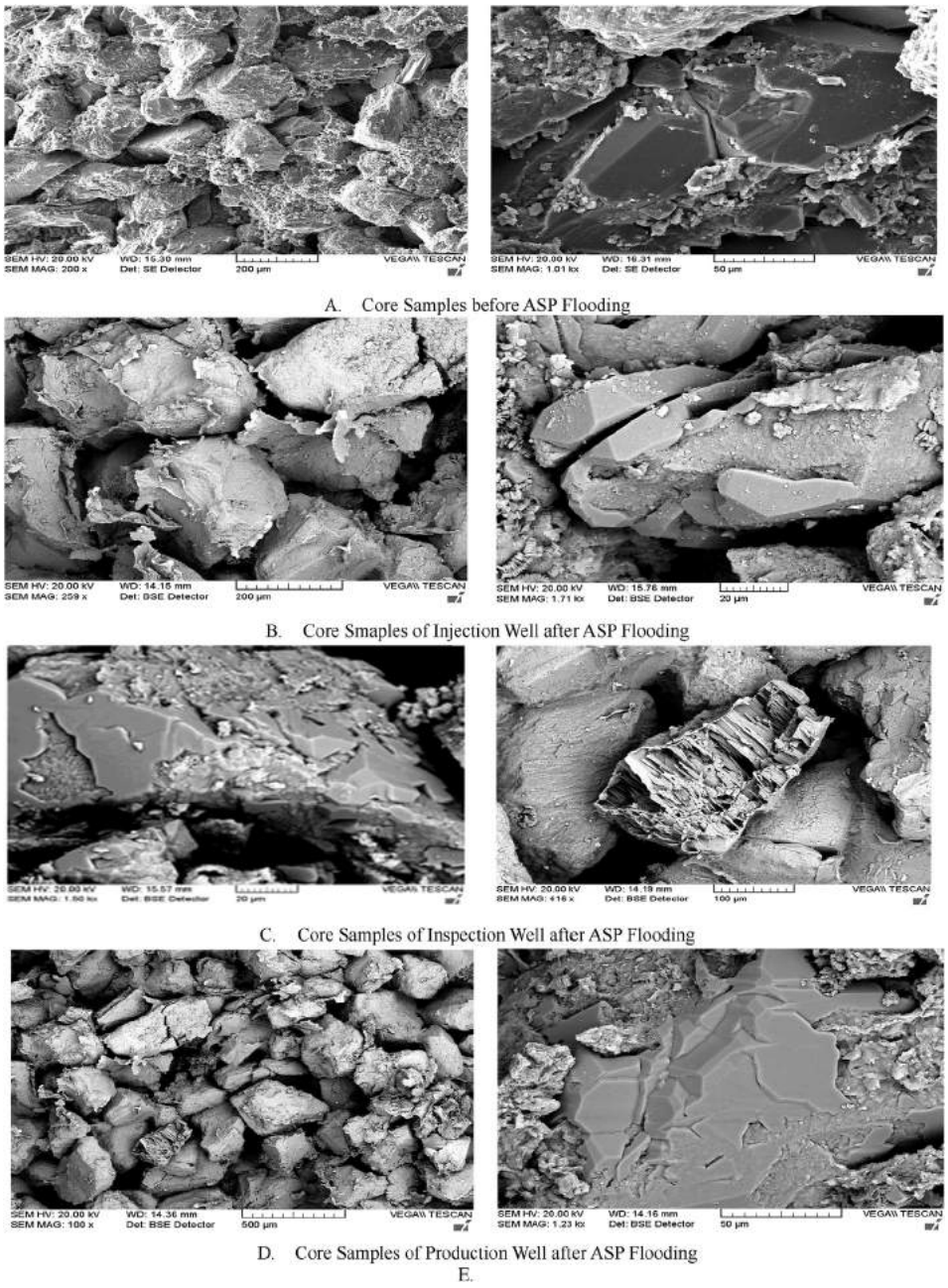

Fig. 7. SEM photos of core samples before and after ASP flooding.

Table 3
Percentage of composition in ASP scaling samples from production well.

	Rod body (%)	Liner (%)	Rotor (%)	Pumping rod (%)
Na_2O	4.065	1.63	2.07	3.90
SiO_2	92.12	85.08	81.45	74.30
CaO	2.92	7.68	15.5	4.69
BaO	0.895	5.61	0	13.37
Al_2O_3	0	0	0	3.74
MgO	0	0	0.98	0

the grains and these grains had smooth surfaces. However, the microscopic features of the core samples from injection wells after ASP flooding (Fig. 7B) included deep corrosion on the surface of mineral granules and some new sediment formation. Parts of the pores or throats were plugged by these sediments, leading to the decline of the permeability. The core samples from inspection wells after ASP flooding (Fig. 7C) also included corrosion on the mineral granules and new sediment formation although less than was found in the injection wells. The connectivity values of the pores and throats were better. Nevertheless, similar to the result of CTS images, the core samples from production wells after ASP flooding (Fig. 7D) also included slight corrosion and the increased sediments, leading to the throat plugging and a decline of connectivity.

Clay minerals, mainly including kaolinite and montmorillonite, were usually located in the pores or at the throats. With the large specific surface area, this type of mineral usually experienced first contact with the externally flowing chemical fluid. Considering the weak intergranular van der Waals forces of kaolinite or montmorillonite, the sodium ions in the flowing fluid were able to have an

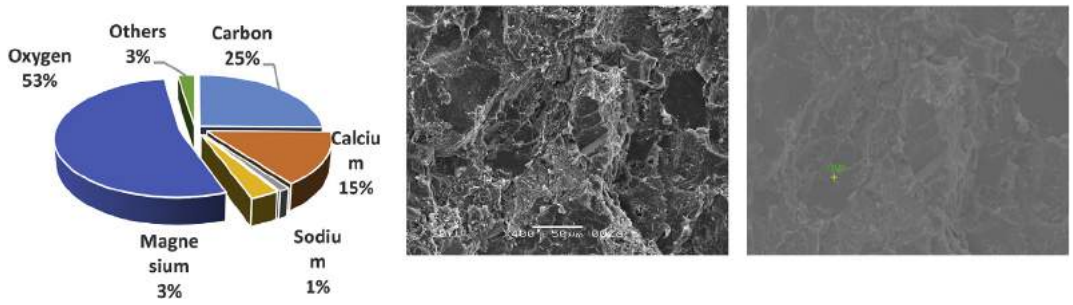

Fig. 8. Percentage of composition and SEM photos in ASP scaling samples from injection well.

Table 4
Ion concentrations of ASP flooding produced fluid.

pH	salinity(mg/L)	cation concentration(mg/L)			Anion concentration(mg/L)				
		Na^++K^+	Ca^{2+}	Mg^{2+}	Cl^-	SO_4^{2-}	CO_3^{2-}	OH^-	HCO^-
9.10	5687.5	1883.9	32.8	7.45	848.59	58.9	720	0.00	2135.7

ion-exchange reaction with the silicon and aluminum ions in the clay minerals, so that a large amount of water molecules and other polar molecules were carried to the crystal layer, causing water swelling of some types of clay minerals, especially montmorillonite, and this clay mineral would be easily corroded. Otherwise, due to mechanical force, the minerals would fracture and the mineral dispersed into flake-shaped granules that migrate into the pores. Meanwhile, the matrix minerals, quartz and feldspar, were relatively stable without cations to exchange and these minerals have lower specific surface areas. Therefore, compared with the alkali consumption of clay minerals such as kaolinite and montmorillonite, the alkali consumptions of quartz and feldspar in flowing fluid were relatively smaller.

4.4. Scaling

Scaling deposits were sampled from an injection well wall and four parts of a production well, including the rod body, liner, rod rotor and pumping rod. Six typical points of each sample were chosen for analysis by XRD and SEM. Simultaneous analysis by XRD and SEM is the most convenient method to determine rock composition and this is the best technique to determine the variety and abundances of clay minerals. The mass fractions of each component in the samples are listed in Fig. 7 and Table 3.

As Fig. 8 shows, the elemental components of the scaling deposits from the injection well were mainly oxygen, carbon and calcium and lesser amounts of magnesium and sodium. These data suggest that calcium carbonate was the main scaling component in the injection well. When the ASP fluid entered into the injection well area, the alkali could react with calcium and magnesium ions to form a precipitate. That is why the components of the scaling deposits from injection wells were mainly calcium. On the other side, the reaction between the alkali and the minerals contributed to the formation of calcium carbonate scaling because the reservoir contained mainly quartz and feldspar. The scaling reduced the permeability of injection well areas.

As seen in Table 3, the differences between the injection well scaling and that of the production wells were mainly silicon dioxide and a small amount of silicate precipitates with carbon, magnesium, barium, etc. The chemical equation is showed below:

$$Ca^{2+}\left(Mg^{2+}, Ba^{2+}\cdots\right) + SiO_3^{2-} = Ca\,SiO_3\downarrow\left(MgSiO_3\downarrow, BaSiO_3\downarrow\cdots\right) \quad (V)$$

Because these types of precipitates formed simultaneously after the change of temperature and pressure, they were mixed and did not have a regular crystalline form detected by X-ray. Due to the different positions of the scaling, the elemental analyses of the samples were a little different. For example, the scaling on the rod body contained barium, while the scaling on the rotor contained magnesium, instead of barium. Aluminum was found in the scaling on the pumping rod, showing that a small amount of this element from a clay mineral was precipitated on the pumping rod after it was dissolved by the strong base ASP flooding.

Table 4 presents the ionic concentrations of the ASP flooding-produced fluid. As listed in this table, the OH^- concentration in the produced fluid was 0 mg/L, showing that the strong base had been consumed by the end of streamline. This indicates that the scaling formed in the production well was not related to OH^-, but was due to other mechanisms.

When strong base ASP flooding fluid entered the injection well areas, it reacted with the reservoir rock, including the clay minerals and a small amount of feldspar and quartz. The OH^- ions from the alkali could corrode the minerals to form SiO_3^{2-} and AlO_2^-. Then, the SiO_3^{2-} micelle might accumulate as orthosilicic acid due to changes of the frictional force or temperature and further dehydrate to form insoluble SiO_2 crystals. Alternatively, the Na^+ ions could have an ion exchange reaction with Ca^{2+} or Mg^{2+} ions or react with SiO_3^{2-} and OH^- to form a silicate and hydroxide precipitate. In addition, the Na^+ ions could react with SiO_3^{2-} or AlO_2^- ions to form different reaction products under different conditions. For example, they could be combined to form albite in suitable geological circumstances leading to a secondary increase of albite. If this occurred it would be rather probable that larger mineral grains would result and that the intergranular pore would become smaller. The other example occurred in the rock fracture. The Na^+ ions reacted with SiO_3^{2-} and AlO_2^- ions to form natrolite under the effect of a hydrothermal process. In summary, the strong base of ASP flooding contacted the surfaces of the silicate rock and reacted with them, forming soluble groups in the flowing fluid. The internal structure of the rock gradually collapsed, and the rock finally disintegrated.

5. Conclusion

The experimental measurements of permeability and porosity were performed to confirm and analyze the different effects to the entire flow pathway of ASP flooding. Based on the results of these measurements, a series of additional experiments, such as

adsorption analysis, SEM, CTS and XRD were conducted to study different influences.

As the amount of absorbed ASP fluid increased, the residual resistance factor became higher and the permeability of material near the injection decreased. This is one of the mechanisms that contributes to the permeability decline near the injection well areas.

Based on the CTS and SEM results and a theoretical assessment, other reasons for the permeability and porosity distribution could be deduced. When the ASP fluid entered the reservoir the high concentration of alkali reacted with the rocks changing the composition of the minerals. Some minerals and cementation at throats were corroded. This could have a large influence on the permeability. Additionally, the high viscosity of the ASP fluid could cause the grains to migrate. In addition, in the inspection well areas between the injection wells and production wells, the elements from the dissolved minerals existed as ions instead forming scale or other participating in other reactions due to the conditions of high temperature and pressure. Therefore, the dominant pathways near the inspection well areas were formed and the permeability increased within these pathways. However, the porosity was affected less than the permeability because the quantity of dissolved minerals was not sufficient to influence the porosity to such degree.

Moreover, the entire system composed of the ASP flooding fluid, reservoir rocks, formation fluid and crude oil is very complex. There were not only chemical reactions between the alkali in ASP flooding and the reservoir minerals but also physical and chemical processes, such as ion-exchange reactions between the alkali and the formation fluid. These processes led to the produced liquid filling with scale-forming ions such as SiO_3^{2-} AlO_2^- Mg^{2+}, Ca^{2+} and OH^-. When the produced fluid flowed near the production wells, the temperature and pressure suddenly dropped, changing the dynamic conditions. In addition, the fluid might become mixed with the formation water that had different pH and hardness values. All of the above factors would influence the equilibrium state of the scale-forming ions. When the equilibrium state was disturbed, the produced fluid would become supersaturated, continuously producing a large amount of aluminosilicate, silicon dioxide and carbonate precipitates. These precipitates have a high possibility of causing serious scaling problems in oil-well facilities by decreasing the permeability of the production well areas.

In summary, these following conclusions can be derived from the results:

1) The permeability and porosity generally decreased in the near-injection-well areas, due to calcium and magnesium scaling in the injection well areas, grain migration and absorption of the alkali and the polymer.
2) The permeability and porosity increased at an intermediate distance, in the inspection well areas because of the dissolution of cementation at the throats and the dominant pathway created by the high viscosity of the ASP fluid. However, the increase of the porosity is not as high as that of the permeability.
3) The permeability and porosity decreased again in the near-production-well areas because of the silicon precipitation caused by the sudden change of the surrounding temperature and pressure. The variation of the porosity was less than that of the permeability.

Acknowledgement

The authors thank the National Natural Science Foundation of China (No. 51174216) and State Key Science & Technology Project of China (Nos. 2011ZX05009-004, and 2011ZX05052) for their financial support to carry out this research. Thank the cooperation of No.2 Oil Production Company, Daqing Oilfield Limited Company. The insightful and constructive comments of the anonymous reviewers are also gratefully acknowledged.

References

Wang, Demin, 2001a. Develop new theory and technique of tertiary production to ensure continuous and stable development of Daqing OilField(I). Pet. Geol. Oilfield Dev. Daqing 20 (3), 1–7.
Alwi Noraliza, et al. "Managing Micro-Emulsion and Scale During ASP Flooding for North Sabah Field EOR." Offshore Technology Conference-Asia. Offshore Technology Conference, 2014.
Alwi Noraliza, et al. "Managing Micro-Emulsion and Scale During ASP Flooding for North Sabah Field EOR." Offshore Technology Conference-Asia. Offshore Technology Conference, 2014.
Li, Bailin, Zhang, Yingying, Dai, Sujuan, et al., 2014. Adsorption properties of ASP flooding system for the central Saertu sub reservoir in Daqing. Journal of Northeast Petroleum University 38 (6), 92–99.
Cai, R., Lindquist, W.B., Um, W., Jones, K.W., 2009. Tomographic analysis of reactive flow induced pore structure changes in column experiments. Adv. Water Resour. 32 (9), 1396–1403.
Li Chen, 2010. Research on Monosandbody Recognition Method and Residual Oil Distribution in PI1-2 in Sanan-5 Areas. Daqing Petroleum Institute, Daqing.
Cheng, Jiecheng, Shi, Mei, Gao, Xiulan, et al., 1992. Effects on resistance factor and residual resistance factor for polymer solution flow through porous media. J. Daqing Pet. Inst. 31–36 (03).
Ciantia, Matteo Oryem, et al., 2015. Effects of mineral suspension and dissolution on strength and compressibility of soft carbonate rocks. Eng. Geol. 184, 1–18.
Colon, C.F.J., Oelkers, E.H., Schott, J., 2004. Experimental investigation of the effect of dissolution on sandstone permeability, porosity, and reactive surface area. Geochim. Cosmochim. Acta 68 (4), 805–817.
Crandell, L.E., Peters, C.A., Um, W., Jones, K.W., Lindquist, W.B., 2012. Changes in the pore network structure of Hanford sediments after reaction with caustic tank wastes. J. Contam. Hydrol. 131 (1–4), 89–99.
Li, Daoshan, Hou, Jirui, Xu, Ruijuan, 2001. Adsorption of components from ASP flooding solution onto reservoir rock of Daqing. Oilfield Chem. (04): 358–361+382.
Denney, Dennis, 2013. Progress and effects of ASP flooding. J. Pet. Technol. 65 (01), 77–81.
Denney, D., Others, 2008. Pump-scaling issues in ASP flooding in Daqing oil field. J. Pet. Technol. 60 (01), 50–52.
Duan, Xianggang, Hou, Jirui, Cheng, Tingting, et al., 2014. Evaluation of oil-tolerant foam for enhanced oil recovery: laboratory study of a system of oil-tolerant foaming agents. J. Pet. Sci. Eng. 122, 428–438.
Emmanuel, S., Berkowitz, B., 2005. Mixing-induced precipitation and porosity evolution in porous media. Adv. Water Resour. 28 (4), 337–344.
Farajzadeh, R., et al., 2013. Effect of continuous, trapped, and flowing gas on performance of Alkaline Surfactant Polymer (ASP) flooding. Ind. Eng. Chem. Res. 52 (38), 13839–13848.
French, Troy R., 1996. A method for simplifying field application of ASP flooding. In: SPE/DOE Improved Oil Recovery Symposium. Society of Petroleum Engineers.
Fu, Qi, Lu, Peng, et al., 2009. Coupled alkali-feldspar dissolution and secondary mineral precipitation in batch systems: 1. New experiments at 200 °C and 300 bars. Chem. Geol. 258, 125–135.
Hao, Hongda, Hou, Jirui, Zhao, Fenglan, et al., 2015. Chromatographic separation of ASP system and its effect on recovery in Daqing second-class oil layer. Oilfield Chem. (01): 119–122+127.
He, Jingang, Song, Kaoping, Kang, Shaodong, et al., 2015. Reservoir pore-throat structure changes after strong base ASP flooding in Daqing oilfield. Pet. Geol. Recovery Effic. (04): 97–102+108.
Hou, Jirui, 2005. Study of Synthetic Effect of Interfacial and Rheologic Properties of ASP Solution on Displacement Oil. Dalian University of Technology, Dalian.
Jia, Zhongwei, Yang, Qingyan, Yuan, Min, et al., 2006. Experimental study on influential factors of ASP displacement efficiency in Daqing oilfield. Acta Pet. Sin. 101–105 (S1).
Kalwar Shuaib Ahmed, et al. "A New Approach to ASP Flooding in High Saline and Hard Carbonate Reservoirs." International Petroleum Technology Conference. International Petroleum Technology Conference, 2014.
Karazincir, Oya, et al., 2011. Scale formation prevention during ASP flooding. In: SPE International Symposium on Oilfield Chemistry. Society of Petroleum Engineers.
Kazempour, M., Sundstrom, E., Alvarado, V., 2012. Geochemical modeling and experimental evaluation of high-pH floods: impact of Water-Rock interactions in sandstone. Fuel 92, 216–230.
Korrani, Aboulghasem Kazemi Nia, Sepehrnoori, Kamy, Delshad, Mojdeh, 2016. Significance of geochemistry in alkaline/surfactant/polymer (ASP) flooding. In: SPE Improved Oil Recovery Conference. Society of Petroleum Engineers.
Kumar, Rahul, Mohanty, Kishore K., 2010. ASP flooding of viscous oils. In: SPE Annual Technical Conference and Exhibition. Society of Petroleum Engineers.
Li, Zihao, Hou, Jirui, Tang, Yongqiang, et al., 2015. Effect of strong base ASP system on reservoir mineral components. Pet. Geol. Oilfield Dev. Daqing 34 (6), 100–105.

Li Mingyuan, 2009. Assessment of CO_2 Storage Potential in Oil/gas Bearing Reservoir in Songliao Basin. Report of the Near Zero Emissions Coal (NZEC).
Liu, Gang, Hou, Jirui, Li, Qiuyan, et al., 2015. Chemicals loss and effective distance of ASP flooding in second-class oil layers. J. China Univ. Pet. 06 (023), 171–177.
Pope, G.A., Wang, Ben, Tsaur, Kerming, 1979. A sensitivity study of micellar/polymer flooding. Soc. Pet. Eng. J. 19 (06), 357–368.
Rathnaweera, T.D., et al., 2015. CO2-induced mechanical behaviour of Hawkesbury sandstone in the Gosford basin: an experimental study. Mater. Sci. Eng. A 641, 123–137.
Sedaghat, M., et al., 2015. Pore-level experimental investigation of ASP flooding to recover heavy oil in fractured five-spot micromodels. In: EUROPEC 2015. Society of Petroleum Engineers.
Sun, Wancheng, 2011. The Study of Anti-Scaling Technology in ASP Flooding in Nanwuqu of Sanan Oilfield. Northeast Petroleum University, Daqing.
Sydansk, R.D., 1982. Elevated-temperature caustic/sandstone interaction: implications for improving oil recovery. SPE J. 22 (4), 453–462.
Um, W., Serne, R.J., Yabusaki, S.B., Owen, A.T., 2005. Enhanced radionuclide immobilization and flow path modifications by dissolution and secondary precipitates. J. Environ. Qual. 34, 1404–1414.
Volokitin, Y.E., et al., 2014. Experimental studies of surfactant adsoption under conditions of ASP flooding at west salym field (Russian). In: SPE Russian Oil and Gas Exploration & Production Technical Conference and Exhibition. Society of Petroleum Engineers.
Wang, Demin, 2001b. Develop new theory and technique of tertiary production to ensure continuous and stable development of Daqing Oilfield(II). Pet. Geol. Oilfield Dev. Daqing 20 (4), 125.
Wang, Demin, 2003. Study on ASP flooding, binary system flooding and mono-system flooding in Daqing oilfield. Pet. Geol. Oilfield Dev. Daqing 22 (3), 1–9.
Wang, Yupu, Cheng, Jiecheng, 2003. The scaling characteristics and adaptability of mechanical recovery during ASP flooding. J. Daqing Pet. Inst. 27 (2), 20–22.
Wang, Xianjun, Wang, Qingguo, 2003. An experimental study on rock/water reactions for alkaline/surfactant/polymer flooding solution used at Daqing. Oilfield Chem. 250–253 (03).
Wang, Yupu, Liu, Yikun, Deng, Qingjun, 2014. Current situation and development strategy of the extra high water cut stage of continental facies sandstone oil fields in China. J. Northeast Pet. Univ. 38 (1), 1–9.
Weatherill, Alan. "Surface development aspects of alkali-surfactant-polymer (ASP) flooding." International Petroleum Technology Conference. International Petroleum Technology Conference, 2009.
Wei, Honghong, Liu, Junlai, Meng, Qingren, 2010. Structural and sedimentary evolution of the southern Songliao Basin, northeast China, and implications for hydrocarbon prospectivity. AAPG Bulletin 94 (4), 533–566.
Wu, Xiaolin, Yin, Yidong, Wu, Guopeng, et al., 2015. Study on the reaction of alkali/surfactant/polymer and reservoir cores in Daqing oilfield. Chem. Eng. Oil Gas 66–72 (05).
Tang, Yongqiang, Hou, Jirui, Li, Chenghui, 2013. Water shut off in a horizontal well: lab experiments with starch graft copolymer agent. J. Pet. Sci. Eng. 108, 230–238.
Yuan, Bin, Han, L., Shan, L., et al., 2011. Evaluation of surfactant-organic phosphonate combination's anti-scaling property. Spec. Petrochem. 28 (1), 70–72.
Yuan, Bin, Ghanbarnezhad Moghanloo, Rouzbeh, Pattamasingh, Purachet, 2015. Applying method of characteristics to study utilization of nanoparticles to reduce fines migration in deepwater reservoirs. In: SPE European Formation Damage Conference and Exhibition. Society of Petroleum Engineers.
Yuan Bin, Rouzbeh G. Moghanloo, and P. Pattamasingh, Analytical Model of Nanofluid Injection to Improve the Performance of Low Salinity Water Flooding in Deepwater Reservoirs, OTC-26363-MS, Offshore Technology Conference Asia, 22–25 March 2016, Kuala Lumpur, Malaysia.
Zhang, Ronglei, et al., 2016. A fully coupled thermal-hydrological-mechanical-chemical model for CO_2 geological sequestration. J. Nat. Gas Sci. Eng. 28, 280–304.
Zhao, Wenzhi, Zou, Caineng, Chi, Yingliu, Zeng, Hongliu, 2011. Sequence stratigraphy, seismic sedimentology, and lithostratigraphic lays: Upper Cretaceous, Sifangtuozi area, southwest Songliao Basin, China. AAPG Bulletin 95 (2), 241–265.